Recent advances in control-based nonlinear vibration testing

G. Raze, G. Abeloos, G. Kerschen
University of Liège, Aerospace and Mechanical Engineering Department,
Allée de la Découverte 9, 4000 Liège, Belgium
e-mail: **g.kerschen@uliege.be**

Abstract
In the virtual prototyping era, it remains crucial to validate the simulation results using experimental tests. In this context, one important assumption at the root of experimental modal analysis, the dominant method used in aerospace, civil and mechanical engineering, is that the structural system behaves linearly. To address this limitation, the idea of control-based nonlinear vibration testing (CBNVT) has recently emerged in the structural dynamics community. CBNVT combines (i) feedback control to stabilize unstable orbits and (ii) path-following techniques to explore - in a systematic and effective manner - the dynamics of the system directly during the experiment, i.e., without the need for a mathematical model of the system. The objective of this paper is twofold, namely (i) to present the existing methods in a unified manner and (ii) to introduce a novel, fully online and derivative-less experimental arclength continuation method.

1 Introduction

Vibration tests of engineering structures are routinely performed in industry and academia. Thanks to the maturity of modal analysis, many useful results can reliably be extracted from tests involving hundreds or even thousands of sensors [1]. One key assumption of modal analysis is linearity, which is increasingly found to be inadequate for real-world structures because they feature high flexibility, advanced materials, friction and contact. Nonlinear structures are challenging to test for a number of reasons [2]. First, the absence of superposition principle makes conventional methods such as phase separation techniques complicated to apply. Second, the same excitation parameters can result in multiple stable and/or unstable responses. Third, these responses can appear or disappear through bifurcations, which mark qualitative changes in the structure under test and lead to the occurrence of jumps between different equilibria.

Control-based methods have been proposed as robust testing approaches to overcome the difficulties associated with nonlinear systems testing. Following the pioneering work of Sieber and Krauskopf on control-based continuation (CBC) [3], other approaches have emerged, such as the use of a phase-locked loop (PLL) [4], and, more recently, the response-controlled stepped-sine testing (RCT) method [5].

The different CBNVT approaches combine two essential elements, namely feedback control to stabilize unstable orbits, and a continuation approach to trace out a curve representative of the dynamic response of the system under test [6]. Yet, CBNVT methods are often presented individually, making it complicated to recognize their common features. In this work, these methods are presented in a unified manner. To overcome some of the limitations presented by state-of-the-art methods, a novel derivative-less experimental CBC approach is also proposed in this work.

This work is organized as follows. Section 2 highlights the issues associated with traditional testing methods and motivates CBNVT. Section 3 then reviews all existing CBNVT approaches, and Section 4 unifies and classifies them. Section 5 presents the novel derivative-less experimental CBC approach. All methods are eventually compared experimentally on an electronic Duffing oscillator in Section 6 before concluding this work in Section 7.

2 Motivation for control-based nonlinear vibration testing methods

Vibration tests are traditionally performed with three types of excitation signals: sinusoidal, impulsive and broadband. In a linear setting, the advantages and drawbacks of these different input signals are well-known. Sinusoidal excitations and the likes are by far the most popular ones for nonlinear vibration testing. For a sinusoidal-type excitation, the two parameters that the user can control are the drive amplitude and frequency. The response of a nonlinear system is generally characterized for multiple values of these parameters. For instance, the drive amplitude may be fixed and the frequency varied. This variation can be continuous or discrete, representing swept-sine (SWS) or stepped-sine (STS) excitations, respectively. The set of points obtained from different frequencies form a curve called the nonlinear frequency response (NFR). Alternatively, one can fix the frequency and vary the drive amplitude and obtain a so-called S-curve (SC).

For illustration, we present the results obtained with such approaches in the case of a Duffing oscillator, a typical academic example qualitatively representative of geometrically nonlinear structures. The response x of this oscillator to an external excitation f is governed by the following ordinary differential equation:

$$m\ddot{x}(t) + c\dot{x}(t) + kx(t) + k_3x^3(t) = f(t), \tag{1}$$

where m, c, k and k_3 are the mass, damping coefficient, linear stiffness and cubic stiffness coefficient, respectively, and an overdot denotes a derivation with respect to time t. Upon using the normalizations $\bar{t} = \omega_0 t$ (with $\omega_0 = \sqrt{k/m}$) and $\bar{x} = \sqrt{k/k_3}x$, Equation (1) can be put into the dimensionless form

$$\bar{x}''(\bar{t}) + 2\zeta_0\bar{x}'(\bar{t}) + \bar{x}(\bar{t}) + \bar{x}^3(\bar{t}) = \bar{f}(\bar{t}), \tag{2}$$

with $\zeta_0 = c/(2\sqrt{km})$, $\bar{f} = \sqrt{k_3/k^3}f$, and a prime denotes derivation with respect to the dimensionless time $\bar{t}$. For the examples shown hereafter, we chose $\zeta_0 = 0.05$.

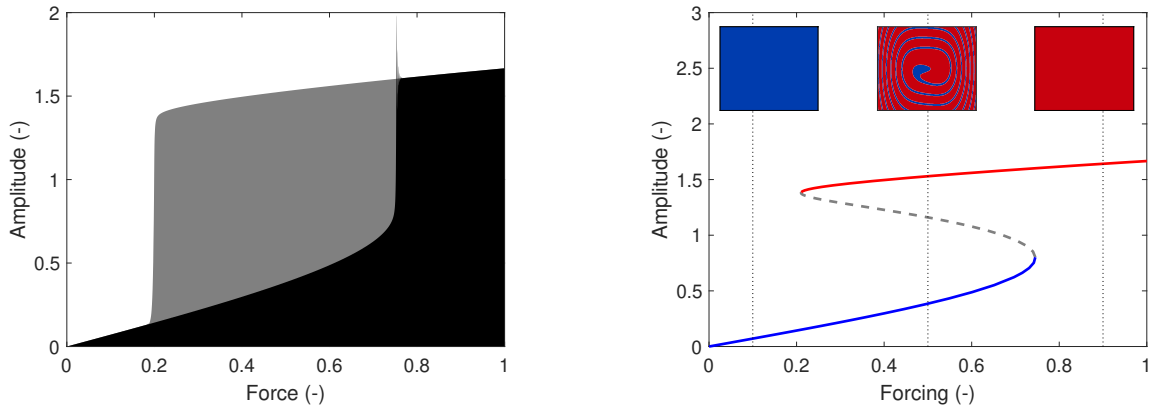

(a) (b)

Figure 1: (a): S-curve of the Duffing oscillator with swept-up (—) and swept-down (—) excitation amplitude at $\bar{\omega} = 1.55$. (b): S-curve of the Duffing oscillator at $\bar{\omega} = 1.55$: upper stable (—), lower stable (—) and unstable (—) branches. Basins of attraction at different forcing conditions are inset in the space of initial conditions $(\bar{x}_0, \bar{x}'_0) \in [-5, 5] \times [-10, 10]$.

We first simulate a sine excitation at fixed frequency $\bar{\omega} = 1.55$ and swept-up amplitude, as shown in Figure 1a. As the forcing amplitude increases, a smooth increase in the response amplitude is observed up to an amplitude $\bar{f} \approx 0.75$, where a sudden jump-up occurs. Conversely, by progressively decreasing the forcing amplitude, a jump-down occurs around $\bar{f} \approx 0.2$. The region delimited by the jump-up and jump-down frequencies is a region of bistability (where the gray area is visible).

The occurrence of jumps indicate that the dynamic response of the system under test has not been thoroughly investigated. These issues are well-known in the nonlinear dynamics community, and are fully treated from a theoretical and numerical point of view. A global understanding of the dynamics of the oscillator can be

obtained with a bifurcation diagram such as the one shown in Figure 1b (obtained with a harmonic balance method coupled with a continuation algorithm [7]), which represents all stable and unstable responses of the Duffing oscillator at the considered forcing frequency. One can observe that there is indeed a region of bistability, wherein the lower and upper stable branches were followed by the responses to amplitude swept-up and swept-down excitations, respectively. These two branches are connected by an unstable one, and they merge near the frequencies at which the jump phenomena occurs. In general, in the bistable region, the stable branch to which the system will settle depends on its initial conditions. This is schematized by the basins of attraction of each attractor at given forcing amplitudes, which are inset in Figure 1b.

A novel class of testing methods, herein called control-based methods, has emerged since the beginning of the last decade. The salient capabilities of these methods are that, through suitable automatic adjustments of the drive signal, they (*i*) allow the experimenter to prescribe given parameters of the system to extract complete experimental bifurcation diagrams (similar to Figure 1b) relying on numerical continuation techniques, and (*ii*) can stabilize the periodic orbits of the system under test. These methods are thus paradigm-shifting for nonlinear vibration testing. In the next sections, we shall present the basics of control-based methods, their different variants, and their core concepts.

3 Overview of the different control-based nonlinear vibration testing approaches

Figure 2 presents the general architecture of a control-based experiment. As in open-loop testing, the system (composed of a structure under test, and a set of actuators and sensors) is excited by a forcing signal. The response of the structure is then analyzed through any of its observables to obtain a representative signal which is fed back to a controller. This controller compares this representative signal to a reference, and adapts the forcing signal to enforce as much as possible an equality between the reference and actual signals. The controller is therefore desired to have a stabilizing action, because it stirs the system toward a reference desired by the experimenter.

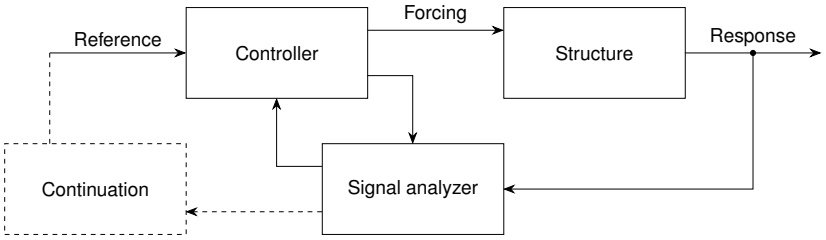

Figure 2: General schematics of a control-based method.

A feedback controller can and generally will completely modify the dynamics of the system. Since the goal of control-based methods is to test the open-loop system under a specific forcing profile, such a modification should be avoided. Another requirement put on the control is thus that it should be *non-invasive*, i.e., the equilibria of the structure in the closed-loop system should be identical to those of the open-loop system. A sufficient condition to enforce this is to subject the closed-loop system to the same excitation as in open-loop conditions (in most cases, a sinusoidal signal). As shall be discussed below, for PLL and RCT, this non-invasiveness requirement is naturally satisfied by the method, allowing the experimenter to freely chose the reference signal. By contrast, for CBC, this requirement is met by adjusting the reference signal through a proper continuation procedure, as depicted by the dashed part of Figure 2.

Having established the common features to all control-based methods, we now describe their main variants, namely CBC, PLL and RCT.

3.1 Control-based continuation

CBC was first proposed by Sieber and Krauskopf [3] in a very general setting by seeking an experimental equivalent to pseudo-arclength continuation. The two key innovations of this work were (a) to use a controller to stabilize the unstable responses of the system under test and (b) to formulate the non-invasiveness condition as a zero problem with measurable functions.

This method is organized around the reference signal, which is set so as to make the control non-invasive by prescribing the force applied on the structure to a preset profile. This non-invasiveness requirement is dealt with by using truncated Fourier series of the signals of interest (performed by the signal analyzer in Figure 2). The difference between the Fourier coefficients of the excitation and a desired excitation profile defines the zero problem. By adjusting the reference signal fed to the controller, this difference can be brought as close to zero as noise allows. To solve this problem, a numerical pseudo-arclength continuation algorithm can be used, where the free parameters are the Fourier coefficients of the reference signals and the bifurcation parameter is the excitation frequency. Since this algorithm relies on Newton-type methods to find the zeros of a residual function, it requires derivatives, which are not known in an experimental setup, but can be approximated using finite differences. Hence, in this work, this original version of the CBC is called CBC-FD.

A substantial simplification of the CBC algorithm was proposed by Barton et al. [8]. They noted that, using a linear time-invariant controller, a single-harmonic input $x_* - x$ (where x is the response of the structure and x_* is the reference signal) to the controller yields a single-harmonic drive. They thus proposed to set the fundamental amplitude of the reference signal to a target value a_*, and to set its other harmonics equal to those of x, thus satisfying the non-invasiveness requirement. They also simplified the continuation algorithm by noting that setting the non-fundamental harmonics of x_* equal to those of x can be performed with a simple Picard iteration scheme, thereby removing the need for experimental finite differences. We refer to this simplified implementation as CBC-A. In [9], it was also shown that adaptive filters can be used as a replacement for the Picard iteration scheme.

The main motivation for using a_* as a bifurcation parameter instead of ω is that it removes the aforementioned folding issue in most cases of interest, provided the control gain are properly chosen [10]. It should be noted that the actual amplitude a will not be exactly equal to the target amplitude a_*, but will tend to it as the controller gains are increased. If this is the case, the S-curve can uniquely be parametrized by $a_* \approx a$, as seen in Figure 1b.

A CBC-A test is performed at a constant frequency ω_*, by progressively varying the value of the target amplitude a_*, obtaining so-called S-curves. Collecting these curves for different target amplitudes gives a surface (in the (ω_*, f, a_*) space) that can be sliced at a constant force level to obtain an NFR. This procedure essentially amounts to fitting experimental data and performing interpolation on the fit.

3.2 Phase-locked loop

PLLs are extensively used in electronics for signal synchronization purposes. Given a reference signal, PLLs are able to adjust the frequency and phase of another signal so as to lock the instantaneous phase difference between these two signals to a prescribed value. Inspired by previous works on autoresonant systems [11, 12], PLLs were introduced to the field of nonlinear vibration testing by Peter and Leine [4].

A PLL test set-up consists of a structure under test, a phase detector (corresponding to the signal analyzer block in Figure 2), a PID controller, and the equivalent of a voltage-controlled oscillator (the two latter being included in the controller block in Figure 2). The difference between a reference θ_* and θ, the phase shift between the response x and the force f, is fed to the PID controller, which automatically adapts the frequency of excitation ω to reach the desired phase. Once ω reaches a steady value, the control is naturally non-invasive and can stabilize unstable responses. By fixing the forcing amplitude f_* and varying the phase θ_*, one can obtain an NFR. Alternatively, by fixing the phase θ_* (typically to obtain phase resonance) and varying the force f_*, one can obtain a constant-phase curve (typically, a phase-resonance backbone curve (BC)).

3.3 Response-controlled stepped-sine testing

The most recent control-based method is the RCT approach, whose basic principles were first drafted in [13] and then elaborated in [5] together with a theoretical justification. Similarly to the CBC-A and PLL, its underlying motivation came from the observation that the frequency-force curves are generally unfolded when the experiment is performed with a constant harmonic amplitude response a_* and varied excitation frequency ω_*. In practice, the harmonic amplitude of the response (typically determined by a Fourier transform in the signal analyzer block in Figure 2) is compared to the target a_* and the forcing amplitude is adjusted iteratively to reach the desired target.

A key argument in favor of this method is that commercial vibration testing software and hardware have the capability to enforce a constant response level [14], therefore offering an off-the-shelf solution to perform CBNVT. For a given target amplitude, the test yields a harmonic force curve (HFC) at different excitation frequencies. Collecting them for multiple target amplitudes, one obtains a harmonic force surface (HFS), and, similarly to CBC-A, NFRs can then be extracted using interpolation of this HFS.

4 Classification of the different control-based nonlinear vibration testing approaches

The two main facets of control-based methods are continuation and control. Both are critical for the success of the experiment. They are discussed hereafter.

4.1 Continuation

As has been discussed in the previous section, tests are mostly performed by varying a parameter and measuring the response of the system under test as this parameter changes. Continuation pertains to the way this parameter is varied, and how it can be used to adequately parametrize the curve forming the set of obtained points. A continuation will be adequate if the curve does not exhibit fold or branching.

Similarly to its numerical counterpart, experimental continuation can be performed in two main variants: natural parameter continuation and arclength continuation. The latter is used by the CBC-FD. As for the former, a series of relevant parameters can be chosen, generally based on how representative they are of the excitation and/or response of the system. To represent the state of a vibrating structure, four distinct variables are generally used:

- f, the amplitude of an external forcing applied to the system,
- ω, the frequency of this forcing,
- a, the amplitude of some harmonic of the response at some point of the structure (typically, the same harmonic as the forcing of the collocated degree of freedom) and
- θ, the phase of this harmonic.

Other variables can of course be considered, but these four are of particular interest in control-based methods. In the most basic set-up, the operator controls f and ω, and a and θ are naturally determined by the evolution of the system (or, in a mathematical setting, they are the unknowns of the problem, whereas f and ω are given parameters). Control-based methods change this paradigm, in the sense that f and/or ω can be automatically adjusted to prescribe a and/or θ as parameters set by the experimenter. But in all cases, there are always two parameters among the four variables that can be set by the operator, while the two remaining variables adapt according to the dynamics of the system.

In addition, one of the two chosen parameters is usually kept constant during a test, while the other is varied. The fixed parameter determines the type of response, whereas the changing parameter is most of the time used as the abscissa when plotting the response of the system. For illustration, Figure 3 represents all possible responses of a Duffing oscillator under tonal excitation as a two-dimensional manifold in the

three-dimensional (ω, f, a) and (ω, f, θ) spaces, together with curves with one of these parameters fixed (which can be seen as "slices" of that manifold).

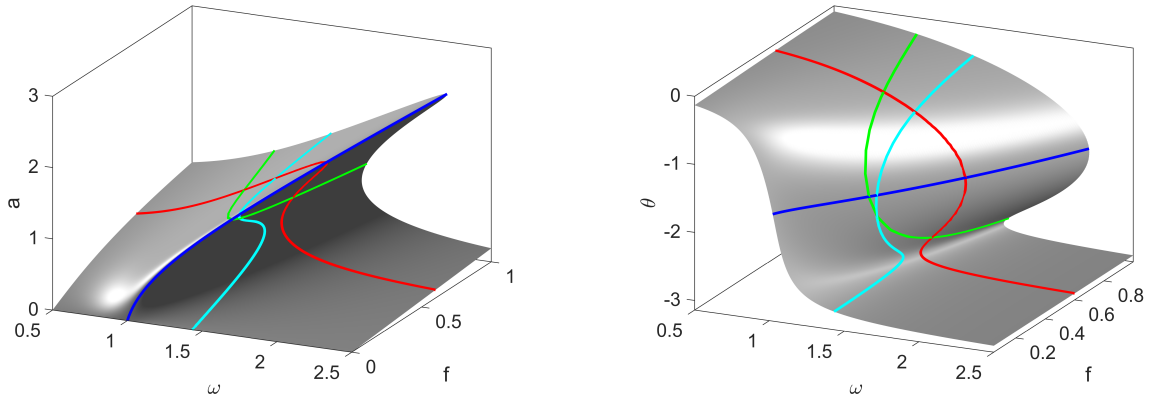

Figure 3: Response manifold of a Duffing oscillator, with constant-f (NFR, —) constant-ω (S-curve, —), constant-a (harmonic force curve, —) and constant-θ (backbone curve, —) curves: (ω, f, a) space (a) and (ω, f, θ) space (b).

With this view in mind, we can classify most of the existing testing methods using periodic excitations following Table 1. In this table, we can distinguish methods that require no, one or two control procedures. By control procedures, we mean, in a broad sense, any procedure that will adjust the input to the systems, using continuous feedback control (for CBC and PLL) or discrete iterative methods (for CBC and RCT). Methods simultaneously imposing f and ω require no control procedure, and are thus always open-loop. Most of the existing control-based methods require just one control procedure, with the exception of the CBC applied to the search of specific phase resonance [15], the CBC combined with the PLL (CBPLL) [16], or the PLL with amplitude control (PLL-A) [17].

Table 1: Classification of the existing experimental natural parameter continuation methods based on the imposed (fixed and parametrization) parameters. Cells in white, light and dark gray require zero, one and two control procedures, respectively, and cells in black are impossible. The brackets indicate which type of curve is obtained.

Varied \ Fixed	f	ω	θ	a
f		Swept sine (S-curve)	PLL (Backbone curve)	
ω	Swept sine (NFR)			RCT (Harmonic force curve)
θ	PLL (NFR)			
a		CBC-A (S-curve)	CBC, CBPLL, PLL-A (Backbone curve)	

Fixing a parameter while varying another one to parametrize the response makes the methods listed in Table 1 inherently equivalent to natural parameter continuation. As such, they are all susceptible to folding issues. This is well-known for the open-loop procedures, but should also be kept in mind when using the control-based methods listed in Table 1.

The only method that does not fit in this table is the CBC-FD, wherein no specific parameter is imposed since this method leverages pseudo-arclength continuation. Folding is almost guaranteed to be absent, which makes this method inherently more robust continuation-wise. Unfortunately, this robustness comes at the expense of substantially longer tests due to the operations required by the method, such as the computation of a Jacobian through finite differences.

4.2 Control

As the continuation procedure progresses through a branch, it is not uncommon to encounter bifurcations and associated stability changes. This is where the control part takes its full importance. Distinctive from continuation, the first role of control is to ensure that all equilibria lying on the branch will be closed-loop stable, but without modifying these equilibria. The second role of control is to automatically adjust ω and/or f to enable continuation.

As outlined in Section 3 and particularly in Figure 2, the main difference between an open-loop test and CBNVT is the presence of a feedback signal driving a controller. Describing mathematically the effect of this controller on stability is beyond the scope of this work, but for illustration, Figure 4 presents the counterpart of Figure 1b when the CBC-A method is used with a simple differential controller, i.e., $\bar{f}(t) = k_d(\bar{x}_*(t) - \bar{x}(t))$ (with a fixed reference signal $\bar{x}_*$ correctly ensuring the non-invasiveness condition). With the differential gain k_d, the open-loop unstable branch can be partially (Figure 4a) or totally (Figure4b) stabilized. When the gain is too small (cf. [10]), the unstable solution co-exists with two stable attractors for which the control is invasive (with $\bar{x}_*$ fixed to make the control non-invasive on the unstable solution).

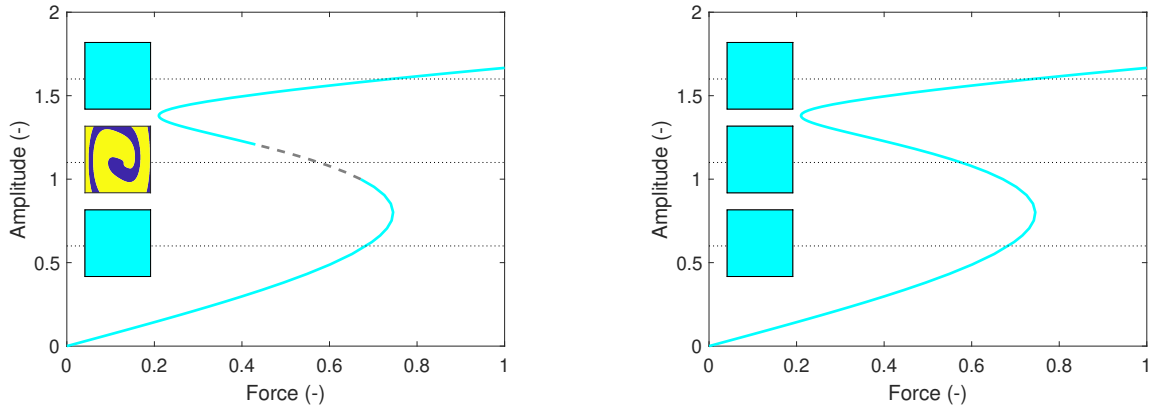

(a) (b)

Figure 4: S-curve of the Duffing oscillator obtained with the CBC-A with a derivative controller at $\bar{\omega} = 1.55$ rad/s: stable (—) and unstable (—) branches for $k_d = 0.4$ (a) and $k_d = 0.5$ (b). Basins of attraction at different target amplitudes are inset in the space of initial conditions $(\bar{x}_0, \bar{x}'_0) \in [-5, 5] \times [-10, 10]$.

5 A novel derivative-less experimental arclength continuation method

According to the discussion in Section 4.1, current control-based methods require a choice from the experimenter. They can either use relatively simple methods such as those presented in Table 1, but the test is then exposed to potential folding issues and the associated possible occurrence of a jump. Alternatively, they can opt for the more general CBC-FD method, which is however more sensitive to noise and makes the test

longer. The main reason for these two downsides is the need for experimental derivatives evaluated through finite differences or Broyden updates.

The purpose of this section is to propose a method which is almost as generic as the CBC-FD method in the sense that it does not assume any parametrization a priori, but which also circumvents the need for experimental derivatives. This procedure, originally presented in [16], is schematized in Figure 5, and called ACBC (arclength CBC) herein. One notes that there exists three feedback paths. Path (*i*) is a classical linear feedback used to stabilize the response. Path (*ii*) is used to ensure the non-invasive character of the control. Finally, path (*iii*) ensures that the proper forcing amplitude is imposed to the structure, which defines a continuation problem. The two latter feedback paths are discussed in more details in what follows.

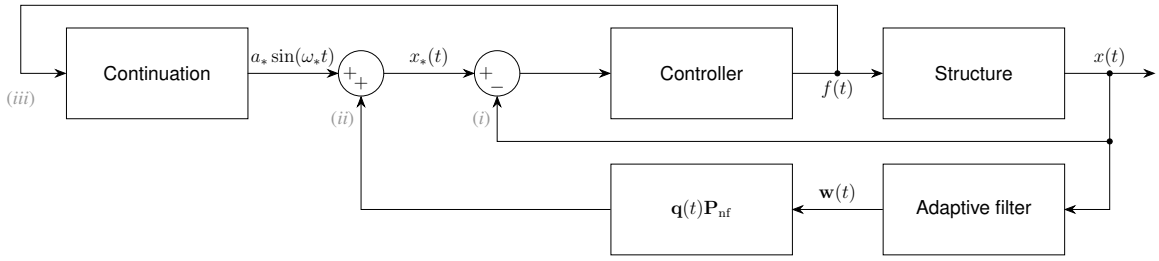

Figure 5: Schematics of the proposed derivative-less CBC method.

5.1 Non-invasive control

As in the CBC, a PID-type controller with a reference signal is used to stabilize the orbits under test. This reference signal is determined based on two criteria. First, its non-fundamental harmonics are set by the non-invasiveness requirements similarly to the CBC-A method. Second, its fundamental harmonic is used together with the excitation frequency to perform continuation.

The force signal is the output of a linear controller, and is desired to be purely sinusoidal to satisfy the non-invasiveness requirement. This is guaranteed as long as the reference and actual signals have identical non-fundamental harmonics, because in this way the signal $x_* - x$ will be a sinusoidal signal at the desired frequency. As in [9], the non-invasive character of the control signal is ensured by the use of adaptive filters. These filters are able to automatically perform a truncated Fourier decomposition of a signal x with h harmonics, i.e.,

$$x(t) \approx \mathbf{q}(t)\mathbf{w}(t), \tag{3}$$

where $\mathbf{w}$ are the $2h+1$ Fourier coefficients, and $\mathbf{q}(t)$ is the associated vector of $2h+1$ harmonic functions

$$\mathbf{q}(t) = \begin{bmatrix} 1 & \sin(\omega t) & \cdots & \sin(h\omega t) & \cos(\omega t) & \cdots & \cos(h\omega t) \end{bmatrix}. \tag{4}$$

The Widrow-Hoff least mean squares (LMS) algorithm can be used to update the Fourier coefficients $\mathbf{w}$ of a signal x through the simple discrete-time law

$$\mathbf{w}((n+1)t_s) - \mathbf{w}(nt_s) = \mu t_s (x(nt_s) - \mathbf{q}(nt_s)\mathbf{w}(nt_s))\mathbf{q}^T(nt_s), \tag{5}$$

where μ is the filter gain and t_s is the sampling time.

Assuming the Fourier coefficients converge to those of x, the control can thus be made non-invasive by defining the target signal as

$$\begin{aligned} x_*(t) &= a_* \sin(\omega_* t) + b_* \cos(\omega_* t) + \mathbf{q}(t)\left(\mathbf{I} - \mathbf{e}_2\mathbf{e}_2^T - \mathbf{e}_{h+2}\mathbf{e}_{h+2}^T\right)\mathbf{w}(t) \\ &= a_* \sin(\omega_* t) + b_* \cos(\omega_* t) + \mathbf{q}(t)\mathbf{P}_{\mathrm{nf}}\mathbf{w}(t), \end{aligned} \tag{6}$$

where $\mathbf{e}_i$ is the i^{th} canonical basis vector of $\mathbb{R}^{2h+1}$. $\mathbf{P}_{\mathrm{nf}}$ can be interpreted as a matrix whose action retains only the non-fundamental harmonics so that, if Equations (3) and (6) hold, the signal $x_* - x$ is mono-harmonic.

5.2 Simplified continuation problem

Having secured the non-invasiveness of the method, three parameters remain to be set by the method, namely a_*, b_* and ω_*. Without loss of generality, one of the Fourier coefficients can be set to zero, say $b_* = 0$. The two remaining unknowns are set by enforcing the fundamental forcing amplitude f to be equal to the target one f_*.

The method can probably be best understood by looking at the force imposed on the structure (which is the output of the controller which has $x_* - x$ as input) as a function of the frequency and target amplitude. On this representation of the HFS depicted in Figure 6, the NFR can be seen as a level set of this surface, where the forcing amplitude f corresponds to the target f_*. In this example, we consider for simplicity infinitely large control gains, such that $a = a_*$. However, we note that the foregoing discussion also holds for finite gains provided they are large enough.

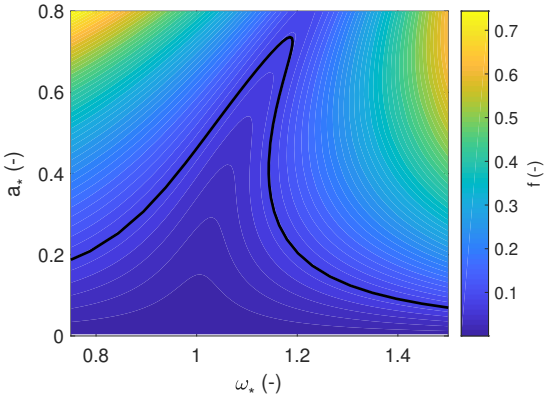

Figure 6: HFS of the Duffing oscillator with the contour level $f = 0.0875$ highlighted (━).

The new approach for experimental continuation leverages this, and is inspired from arclength continuation. Because the NFR is one-dimensional in the (ω_*, a_*) space, a sufficiently small ellipse with semi-axes $\Delta\omega$ and Δa and centered on a point of the branch intersects it twice, as depicted in Figure 7a. The intersections are characterized by $f - f_* = 0$, whereas every other point of the ellipse does not (in general) satisfy this equality. The continuation procedure can thus be formulated as follows: given a current point (ω_n, a_n) and an ellipse centered around it in the (ω_*, a_*) space, the next point of the NFR (ω_{n+1}, a_{n+1}) is found as the intersection of the ellipse and the level set where $f = f_*$, as seen in Figure 7b. To do so, the procedure sweeps along the ellipse by automatically varying the eccentric anomaly α of a point on the ellipse. The procedure can then be repeated using an ellipse centered around every new point, which eventually yields a set of points on the NFR.

A key advantage of this approach is that the harmonic forcing amplitude can easily be measured online, and there are several strategies to find the eccentric anomaly that solves the zero problem $f - f_* = 0$ without need for experimental derivatives. A first simple possibility consists in sweeping the angle $\alpha(t)$ at a constant rate r_α until $f = f_*$. A continuous integral control law $\dot{\alpha} = -k_\alpha(f - f_*)$ can also be used. The sweeping law can be chosen freely by the user depending on their preference, and is denoted by $\dot{\alpha} = s(f - f_*)$ in the sequel. The sweeping rate r_α or gain k_α should be high for a fast continuation, but is nevertheless limited by the system's transients, as well as the adaptive filters speed to guarantee a non-invasive control.

5.3 The algorithm

Algorithm 1 summarizes the proposed ACBC procedure. In this implementation, the prediction is made with the previous converged value of α, which amounts to implementing a secant predictor. ρ represents a relative tolerance, and $\sigma < 1$ is a factor that makes the algorithm stop sweeping in more strict conditions then the convergence check in order to anticipate transient effects.

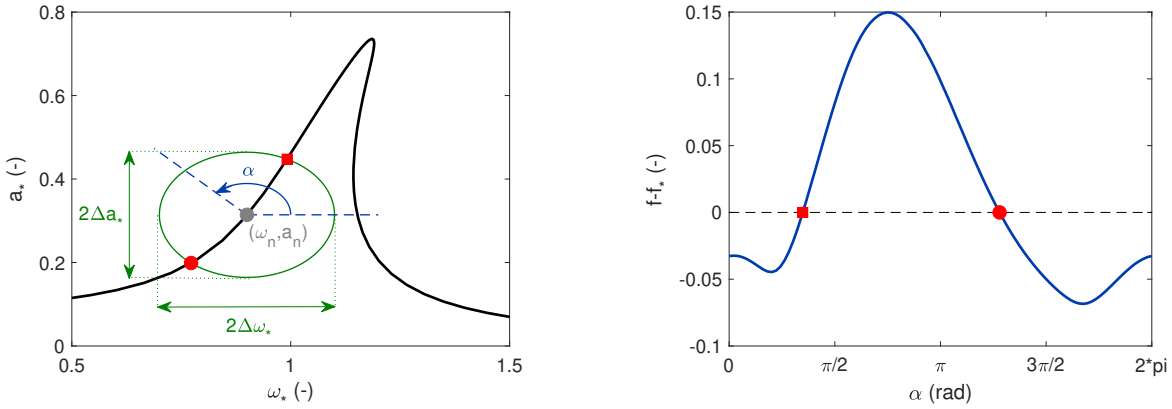

(a) (b)

Figure 7: (a): Definition of the ellipse (—) built around a given point (•) used for the ACBC method to obtain points (•, ■) on the NFR (—) at $\bar{f} = 0.0875$. (b): Profile of the function $f - f_*$ along the ellipse, whose roots (•, ■) correspond to the intersection of the ellipse with the NFR.

The proposed algorithm is equivalent to the CBC-FD in terms of generality of the continuation approach, as it does not make any assumption on the unfolding property of a parameter. A key advantage of this approach is its derivative-free nature, brought by the combined use of the adaptive filters and the arclength continuation procedure in a two-dimensional space. Furthermore, this algorithm is quite simple and can be realized in a fully online way.

6 Illustration with an electronic Duffing oscillator

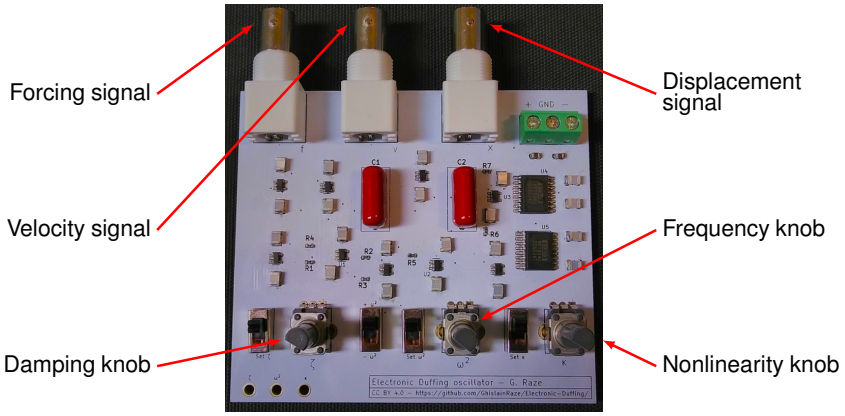

Figure 8: Picture of the electronic Duffing oscillator.

In this study, an electronic circuit that replicates the behavior of a Duffing oscillator is used. This circuit is shown in Figure 8 and described in more details in [18]. The parameters c, k and k_3 (cf. Equation (1)) of the electronic Duffing oscillator can be tuned with knobs (potentiometers). Their theoretical and identified values are reported in Table 2.

All methods were programmed in a fully online way with dSPACE RTI for Simulink and uploaded to a MicroLabBox from dSPACE, except for the RCT whose implementation was directly available in Siemens TestLab using a Scadas Mobile.

Most parameters were tuned on a trial and error basis. A fine-tuning toward optimal performance was not sought given the very large number of parameters and their variety. The results given therein are thus not to be interpreted as the best each method can yield, but rather as an order of idea of how they compare.

Algorithm 1 Derivative-free arclength continuation for CBC experiment.

Input: $\omega_0, a_0, \Delta\omega, \Delta a$ selected by the user.
$n \leftarrow 0$
$\alpha \leftarrow 0$
loop
    Prediction
    $(\omega_*, a_*) \leftarrow (\omega_n + \Delta\omega\cos(\alpha), a_n + \Delta a\sin(\alpha))$
    Wait t_{steady} seconds for steady-state
    Correction
    while $|f - f_*| > \sigma\rho f_*$ **do**
        $\dot{\alpha} = s(f - f_*)$
        $(\omega_*, a_*) \leftarrow (\omega_n + \Delta\omega\cos(\alpha), a_n + \Delta a\sin(\alpha))$
    end while
    Wait t_{steady} seconds for steady-state
    Convergence check
    if $|f - f_*| \leq \rho f_*$ **then**
        $(\omega_{n+1}, a_{n+1}) \leftarrow (\omega_*, a_*)$
        $n \leftarrow n + 1$
    end if
end loop

Table 2: Theoretical and identified parameters of the electronic Duffing oscillator.

Parameter	Theoretical value	Identified value
m (s^2)	10^{-4}	1.0461×10^{-4}
c (s)	1.3×10^{-4}	1.4231×10^{-4}
k (-)	1.923	1.8099
k_3 (V^{-2})	0.9887	1.0077

We focus on measuring an NFR at a specific excitation $f = 0.03$ V between 50 and 200 rad/s. Table 3 gathers the times needed to perform each experiment. Stepped methods (CBC-FD, CBC-A, ACBC and RCT) require the definition of steps $\Delta\omega_*$ and Δa_*, which are based on the desired resolution of the NFR. As for methods were the input parameter is swept (SWS and PLL), the sweep rate was adjusted to make the total test time as long as that of the fastest stepped method.

Table 3: Times taken by each test for the primary resonance.

Method	Total time (s)	Time per point (s)
SWS (up and down)	240	/
CBC-FD	396	4.96
CBC-A (Picard)	453	0.62
CBC-A (Adaptive)	397	0.55
ACBC	240	3.19
PLL	240	/
RCT	7 847	10.13

To start off this analysis, Figure 9 shows the velocity signal NFR directly obtained from methods that ran without issues, namely, the SWS, PLL and ACBC approaches. The agreement between the two latter is excellent. Some discrepancies are observable with the SWS data: as usual, transient effects are the cause for a slightly lower peak amplitude. We also note that the SWS data includes higher harmonics as well. The PLL test experiences large noise at low frequency, which can be mitigated by selecting lower gains for the

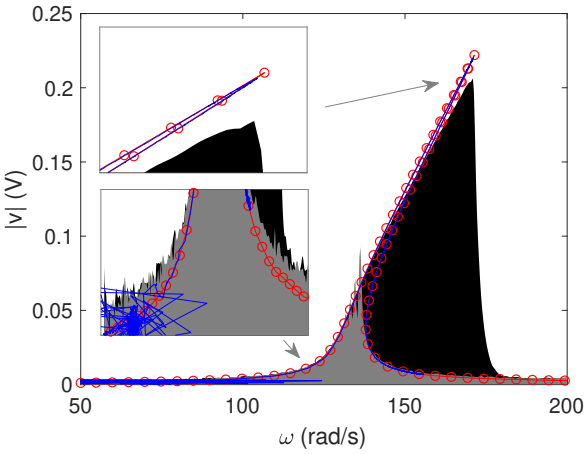

Figure 9: NFR (fundamental harmonic amplitude of the velocity signal) of the electronic Duffing oscillator obtained with the PLL (—) and ACBC (—) methods. The envelope of the (multi-harmonic) response for swept-up (—) and swept-down (—) sine excitations is also shown for comparison.

PI controller; however, doing so destabilized a part of the open-loop unstable branch of the resonance peak. This noise can be explained by the fact that at such low frequencies, the phase is relatively insensitive to the frequency, i.e. $\mathrm{d}\theta/\mathrm{d}\omega$ is small. Conversely, $\mathrm{d}\omega/\mathrm{d}\theta$ is large, meaning that the excitation frequency is very sensitive to small errors in the phase. Small phase noise can thus translate into large frequency noise.

The results obtained with the CBC-FD method are compared to those of the ACBC method in Figure 10. Convergence issues were encountered with the former method in the vicinity of the resonance peak, requiring to restart the method from the high-frequency limit (200 rad/s) to approach the peak from both sides.

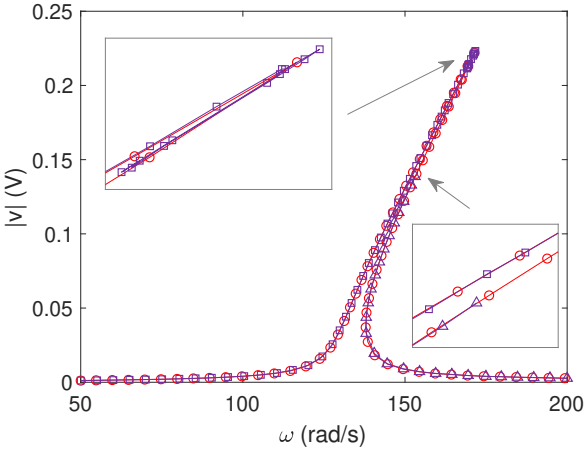

Figure 10: NFR (fundamental harmonic amplitude of the velocity signal) of the electronic Duffing oscillator obtained with the ACBC (—) and CBC-FD (—, □: starting from 50 rad/s, △: starting from 200 rad/s) methods.

The difficulties encountered with CBC-FD are most likely due to two main causes. First, owing to the small damping of the oscillator, the NFR curve experiences a sharp turn near the fold bifurcation. As a consequence, the pseudo-arclength method can struggle to converge to the curve during a correction phase. This issue could be solved by using an arclength continuation scheme, or taking smaller steps. The second issue is linked to the use of finite differences, and again, is mostly problematic in the vicinity of the resonance peak. Indeed, close to this peak, the residual function varies extremely rapidly and has a large curvature (as will also be illustrated by Figure 11a). Smaller finite difference steps could have been taken, but this would shift the issues to zones away from resonance, where the residual function is much less sensitive to variations

in the input, and where large enough finite difference steps need to be taken to overcome noise. This issue could be solved using an adaptive finite difference step by, e.g., prescribing an ideal change in the residual function (suitably larger than the noise level).

As explained in the respective works where the methods were proposed, both CBC-A and RCT obtain a collection of response curves that can be combined into a response surface. NFR curves can be extracted from this surface by slicing it with a plane characterized by $|f| = f_*$, which essentially amounts to performing interpolation on experimental data. An off-the-shelf solution used in this work was to use the `griddedInterpolant` function in Matlab to fit the measured force and amplitude as 2D spline functions of the frequency and target amplitude, as $\hat{f}(\omega_*, a_*)$ and $\hat{a}(\omega_*, a_*)$, respectively (where a hat denotes an interpolated function). The curves satisfying $\hat{f}(\omega_*, a_*) - f_* = 0$ were then found using the `fimplicit` function. Figure 11a shows such curves obtained for the CBC-A. Points of these curves were finally fed to the fitted function $\hat{a}(\omega_*, a_*)$ to obtain the NFR curve.

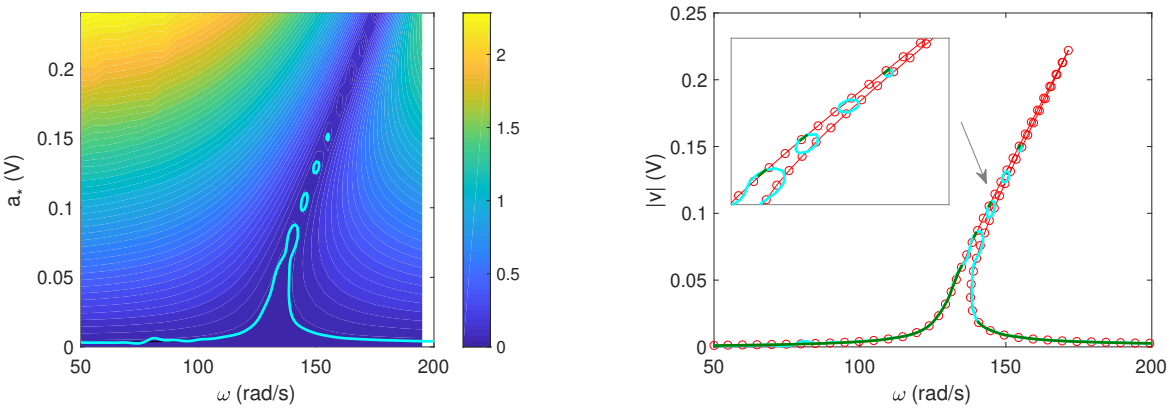

(a) (b)

Figure 11: Contour plot of the measured force for the CBC-A test with the contour $\hat{f} = 0.03$ V highlighted (—) (a), and NFR (fundamental harmonic amplitude of the velocity signal) of the electronic Duffing oscillator obtained with the ACBC method (—) and estimated with the CBC-A (—) and RCT (—) methods (b).

The results of the CBC-A and RCT obtained with this method are compared to those of the ACBC in Figure 11b. While the interpolated NFRs are close to the one from ACBC away from the resonance peak, there is a clear discrepancy between the two types of results in the vicinity of the peak. This issue is mainly due to the interpolation, and to an insufficient resolution of the ω_*, a_* test grid: near resonance, the function $\hat{f}(\omega_*, a_*)$ varies very rapidly and requires a very fine resolution for the interpolation to be correct. This can be solved using either a finer grid (but this requires a longer test time), or using an adaptive sampling strategy instead of a regular grid. Figure 12 supports this hypothesis for the CBC-A by showing the results obtained by narrowing the test frequencies from 120 to 180 rad/s with steps of 2 rad/s, and amplitude steps of 0.05 V, effectively doubling the resolution in both directions. Clearly, the agreement between both methods is improved, at the expense of a longer test time (increasing by a factor 4) for the CBC-A. The interpolation with the CBC-A still inadequately represents a range of about 10 rad/s near the resonance peak, though.

As for the RCT results, it can be observed in Figure 11a that the NFR looks incomplete, which is due to stability issues encountered during the test. The control algorithm was not able to enforce the desired response amplitude for some values of ω_* and a_*, and points where the relative error between the desired and actual harmonic amplitude exceeded 20% were discarded, explaining the incomplete aspect of the NFR and the rather long total time taken by the RCT method. Since the control scheme comes from a commercial software which is the same as that used in [5], an implementation error cannot explain this issue. Different parameters were also tried out without success, as a zone of instability always appeared in the same range.

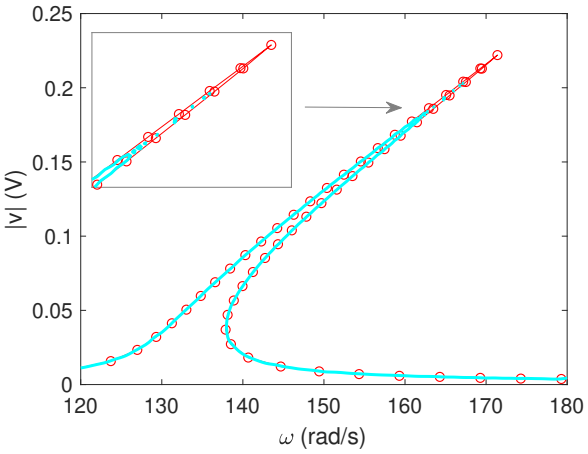

Figure 12: NFR (fundamental harmonic amplitude of the velocity signal) of the electronic Duffing oscillator obtained with the ACBC method (—) and estimated with the CBC-A method with higher frequency and amplitude resolution (—).

7 Conclusion

CBNVT is a relatively novel paradigm that offers appealing features to obtain a global understanding of the nonlinear dynamics of a system under test. By combining a proper continuation procedure and non-invasive control scheme, it is possible to obtain full experimental bifurcation diagrams encompassing open-loop unstable responses.

This work reviewed the different CBNVT approaches and classified them in an unified framework. Moreover, a novel derivative-less arclength CBC approach, termed ACBC, was proposed, being both quick and robust. All methods were illustrated with an electronic Duffing oscillator. Thanks to the excellent repeatability of this set-up, consistent results were observed with nearly each method. Small discrepancies were observed with the CBC-A due to resolution issues, and instabilities with the RCT prevented a full obtention of an NFR.

Acknowledgements

Ghislain Raze is a Postdoctoral Researcher of the Fonds de la Recherche Scientifique - FNRS which is gratefully acknowledged.

References

[1] D. J. Ewins, *Modal Testing: Theory, Practice and Application*. John Wiley & Sons, 2009.

[2] K. Worden and G. R. Tomlinson, *Nonlinearity in Structural Dynamics*. IOP Publishing Ltd, 2001. [Online]. Available: http://stacks.iop.org/0750303565

[3] J. Sieber and B. Krauskopf, "Control based bifurcation analysis for experiments," *Nonlinear Dynamics*, vol. 51, no. 3, pp. 365–377, feb 2008. [Online]. Available: http://link.springer.com/10.1007/s11071-007-9217-2

[4] S. Peter and R. I. Leine, "Excitation power quantities in phase resonance testing of nonlinear systems with phase-locked-loop excitation," *Mechanical Systems and Signal Processing*, vol. 96, pp. 139–158, nov 2017. [Online]. Available: https://linkinghub.elsevier.com/retrieve/pii/S0888327017302005

[5] T. Karaağaçlı and H. N. Özgüven, "Experimental modal analysis of nonlinear systems by using response-controlled stepped-sine testing," *Mechanical Systems and Signal Processing*, vol. 146, p. 107023, jan 2021. [Online]. Available: https://linkinghub.elsevier.com/retrieve/pii/S088832702030409X

[6] G. Abeloos, F. Müller, E. Ferhatoglu, M. Scheel, C. Collette, G. Kerschen, M. Brake, P. Tiso, L. Renson, and M. Krack, "A consistency analysis of phase-locked-loop testing and control-based continuation for a geometrically nonlinear frictional system," *Mechanical Systems and Signal Processing*, vol. 170, no. October 2021, p. 108820, may 2022. [Online]. Available: https://linkinghub.elsevier.com/retrieve/pii/S0888327022000188

[7] T. Detroux, L. Renson, L. Masset, and G. Kerschen, "The harmonic balance method for bifurcation analysis of large-scale nonlinear mechanical systems," *Computer Methods in Applied Mechanics and Engineering*, vol. 296, pp. 18–38, nov 2015. [Online]. Available: https://linkinghub.elsevier.com/retrieve/pii/S0045782515002297

[8] D. A. W. Barton and J. Sieber, "Systematic experimental exploration of bifurcations with noninvasive control," *Physical Review E*, vol. 87, no. 5, p. 052916, may 2013. [Online]. Available: https://link.aps.org/doi/10.1103/PhysRevE.87.052916

[9] G. Abeloos, L. Renson, C. Collette, and G. Kerschen, "Stepped and swept control-based continuation using adaptive filtering," *Nonlinear Dynamics*, vol. 104, no. 4, pp. 3793–3808, jun 2021. [Online]. Available: https://link.springer.com/10.1007/s11071-021-06506-z

[10] S. Tatzko, G. Kleyman, and J. Wallaschek, "Continuation methods for lab experiments of nonlinear vibrations," *GAMM-Mitteilungen*, vol. 46, no. 2, pp. 1–13, jun 2023. [Online]. Available: https://onlinelibrary.wiley.com/doi/10.1002/gamm.202300009

[11] V. Babitsky, "Autoresonant mechatronic systems," *Mechatronics*, vol. 5, no. 5, pp. 483–495, aug 1995. [Online]. Available: https://linkinghub.elsevier.com/retrieve/pii/0957415895000262

[12] S. Mojrzisch, J. Wallaschek, and J. Bremer, "An Experimental Method for the Phase Controlled Frequency Response Measurement of Nonlinear Vibration Systems," *PAMM*, vol. 12, no. 1, pp. 253–254, dec 2012. [Online]. Available: https://onlinelibrary.wiley.com/doi/10.1002/pamm.201210117

[13] M. Link, M. Boeswald, S. Laborde, M. Weiland, and A. Calvi, "Non-linear experimental modal analysis and application to satellite vibration test data," *ECCOMAS Thematic Conference - COMPDYN 2011: 3rd International Conference on Computational Methods in Structural Dynamics and Earthquake Engineering: An IACM Special Interest Conference, Programme*, no. May 2014, 2011.

[14] A. Carrella, "Introduction to Environmental Testing," 2020. [Online]. Available: https://community.sw.siemens.com/s/article/simcenter-testlab-vibration-control

[15] L. Renson, D. A. Barton, and S. A. Neild, "Experimental tracking of limit-point bifurcations and backbone curves using control-based continuation," *International Journal of Bifurcation and Chaos*, vol. 27, no. 1, pp. 1–19, 2017. [Online]. Available: https://www.worldscientific.com/doi/abs/10.1142/S0218127417300026

[16] G. Abeloos, "Control-based methods for the identification of nonlinear structures," Ph.D. dissertation, University of Liège, 2022. [Online]. Available: https://hdl.handle.net/2268/295414

[17] L. Woiwode and M. Krack, "Experimentally uncovering isolas via backbone tracking." *Journal of Structural Dynamics*, pp. 122–143, 2024. [Online]. Available: https://popups.uliege.be/2684-6500/index.php?id=180

[18] G. Raze, "An electronic Duffing oscillator," 2024. [Online]. Available: https://github.com/GhislainRaze/Electronic-Duffing